Chapter 10
Wavelet Transform Analysis of Turbulence

The phenomenon of turbulence was discovered physically and is still largely unexplored by mathematical techniques. At the same time, it is noteworthy that the physical experimentation which leads to these and similar discoveries is a quite peculiar form of experimentation; it is very different from what is characteristic in other parts of physics. Indeed, to a great extent, experimentation in fluid dynamics is carried out under conditions where the underlying physical principles are not in doubt, where the quantities to be observed are completely determined by known equations. The purpose of the experiment is not to verify a proposed theory but to replace a computation from an unquestioned theory by direct measurements. Thus wind tunnels are, for example, used at present, at least in part, as computing devices of the so-called analog type (or, to use a less widely used, but more suggestive, expression proposed by Wiener and Caldwell: of the measurement type) to integrate the nonlinear partial differential equations of fluid dynamics.

John von Neumann

The use of the wavelet transform for the study of turbulence owes absolutely nothing to chance or fashion but comes from a necessity stemming from the current development of our ideas about turbulence. If, under influence of the statistical approach, we had lost the need to study things in physical space, the advent of supercomputers and the associated means of visualization have revealed a zoology specific to turbulent flows, namely, the existence of coherent structures and their elementary interactions, none of which are accounted for by the statistical theory.

Marie Farge

10.1 Introduction

Considerable progress has been made over the last three decades in our understanding of turbulence through new developments of theory, experiment, and computation. More and more evidence has been accumulated for the physical description of turbulent motions in both two and three dimensions. Consequently,

L. Debnath, F.A. Shah, *Wavelet Transforms and Their Applications*,
DOI 10.1007/978-0-8176-8418-1_10

turbulence is now characterized by a remarkable degree of order even though turbulence is usually defined as disordered fluid flows. In spite of tremendous progress, there are still a number of open questions and unsolved problems. These include coherent structures and intermittency effects, singularities of the Navier–Stokes equations, non-Gaussian statistics of turbulent flows, perturbations to the small scale produced by nonisotropic, non-Gaussian, and inhomogeneous large-scale motions, and measurements and computations of small-scale turbulence. No complete theory is yet available for the problem of how the eddy structure of turbulence evolves both under the action of mean distortion and even during the mutual random interaction of eddies of different sizes or scales.

Most of the progress has been based on the Navier–Stokes equations combined with the Fourier transform analysis. However, there are certain major difficulties associated with the Navier–Stokes equations. First, in three dimensions, there are no general results for the Navier–Stokes equations on existence of solutions, uniqueness, regularity, and continuous dependence on the initial conditions. However, such results exist for the two-dimensional Navier–Stokes equations. Second, there are indications that solutions of three dimensional Navier–Stokes equations can be singular at certain places and at certain times in the flow. Third, another difficulty arises from the strong nonlinear convective term in the equation. This nonlinearity leads to an infinite number of equations for all possible moments of the velocity field. This system of equations is very complicated in the sense that any subsystem is always nonclosed because it contains more unknowns than the number of equations in a given subsystem. For example, the dynamical equation for second-order moments involves third-order moments, that for third-order moments involves fourth-order moments, and so on. This is the so-called closure problem in the statistical theory of turbulence. This is perhaps the major difficulty of the turbulence theory. For any physical system with strong interaction, such as turbulent flows, it is not easy to guess what kind of closure is consistent with the Navier–Stokes equations. Various closure models for turbulence, including the quasi-normal model (see Monin and Yaglom 1975) have been suggested. They are hardly consistent with physical analysis, experimental measurements, and, more recently, with direct numerical simulations (DNSs) of turbulence. Fourth, in the limit as $\nu \to 0$ ($R \to \infty$), the nature of the Navier–Stokes equations changes because the nonlinear convective term dominates over the linear viscous term. Therefore, for fully developed turbulence, as $R \to \infty$, the second-order viscous term vanishes. Consequently, the second-order Navier–Stokes equations reduce to the first-order Euler equations. Thus, a slightly viscous fluid flow can lead to a *singular perturbation* of the inviscid fluid motions. Mathematically, the Navier–Stokes equations lead to a singular perturbation problem. Another major difficulty in modeling the structure and dynamics of turbulence is the wide range of length and time scales over which variations occur. However, in recent years, a broad class of self-similar dynamical processes has been developed as a possible means of characterizing turbulent flows.

Traditionally, the Fourier transform approach to turbulence has been successful due to the fact that the Fourier transform breaks up a function (or signal) into different sine waves of different amplitudes and wavenumbers (or frequencies).

In fact, the classical theory of turbulent flows was developed in the Fourier transform space by introducing the Fourier energy spectrum $\hat{E}(k)$ of a function $f(x)$ in the form

$$\hat{E}(k) = \left|\hat{f}(k)\right|^2. \tag{10.1.1}$$

However, $\hat{E}(k)$ does not give any local information on turbulence. Since $\hat{f}(k)$ is a complex function of a real wavenumber k, it can be expressed in the form

$$\hat{f}(k) = \left|\hat{f}(k)\right| \exp\{i\theta(k)\}. \tag{10.1.2}$$

The phase spectrum $\hat{\theta}(k)$ is totally lost in the Fourier transform analysis of turbulent flows, and only the modulus of $\hat{f}(k)$ is utilized. This is possibly another major weakness of the Fourier energy spectrum analysis of turbulence since it cannot take into consideration any organization of the turbulent field. Also, the rate of energy dissipation is distributed very intermittently in both space and time. This is usually modeled by the breakdown of eddies, and the flux of energy is assumed to flow from larger to smaller eddies so that the turbulence is generated to small scales, where it is dissipated by viscosity. Evidently, there is a need for introducing a flux of kinetic energy which also depends on position. For a real description of real turbulence, there is a need for a representation that decomposes the flow field into contributions of different length scales, different positions, and different directions.

The idea of a hierarchy of vortices is usually employed in the study of turbulence. Combined with the theory of scales, a model of turbulence as a vortex system of different sizes with random amplitude functions leads to the statistical description of turbulence. Kolmogorov (1941a,b) used this approach to derive his famous spectral law for isotropic and homogeneous turbulence. In this idea of a hierarchy of vortices, the velocity field can be represented in terms of Fourier integral transforms. This representation seems to be unsatisfactory for the following reason. Each Fourier component in the decomposition of the velocity vector potential corresponds to a coherent vortex structure over the entire space. But the strong nonlinear interaction of the spatial temporal modes in turbulence results in the effect that periodic solutions representing coherent vortex systems are not typical structural components of the turbulent motion. The processes involving energy transfer, deformation, and vortex decomposition are described by the local conditions of the turbulent flow.

Therefore, the Fourier transform analysis does not have the ability to provide a local description of turbulent flows. In fact, the scale, position, and direction involved in the flow field are completely lost in this analysis. Moreover, the Fourier transform cannot describe the multifractal structure of fully developed turbulence. The new method of wavelet transform analysis may enable representation of quantities that depend on scale, position, and direction, and hence it has the ability to give local information about the turbulent flows.

In a series of papers, Farge and her associates (Farge 1992; Farge et al. 1992, 1990a; Farge and Holschneider 1989, 1990; Farge et al. 1990b, 1996, 1999a,b; Farge and Rabreau 1988, 1989) introduced new concepts and ideas to develop a new and modern approach to turbulence based on the wavelet transform analysis. They showed that the wavelet transform can be used to define local energy density, local energy spectrum, and local intermittency, to determine singularities, and to find extrema of derivatives at different positions and scales. These studies reveal that both wavelet and fractal analyses seem to be very useful and effective mathematical tools for investigating the self-similarity, coherent structures, intermittency, and local nature of the dynamics and other features of turbulent flows. Meneveau (1991, 1993) initiated wavelet transform analysis for the study of time-dependent three-dimensional computations of the velocity field in a turbulent flow. He also provided the first direct evidence that energy flows from small to large scales in some regions of turbulence. This is a remarkable new phenomenon that cannot be studied by using Fourier transform analysis.

This chapter is devoted to a brief discussion of Fourier transform analysis and the wavelet transform analysis of turbulence based on the Navier–Stokes equations. Included are fractals, multifractals, and singularities in turbulence. This is followed by Farge's and Meneveau's wavelet transform analyses of turbulence in some detail. Special attention is given to the adaptive wavelet method for computation and analysis of turbulent flows. Many references related to applications of the wavelet transform in turbulence are cited in the bibliography.

10.2 Fourier Transforms in Turbulence and the Navier–Stokes Equations

It is well known that a Fourier transform decomposes a function or a signal $f(x)$ into different sine waves of different amplitudes and wavelengths. In general, the Fourier transform of a signal $f(x)$ can be expressed as

$$\hat{f}(k) = \left|\hat{f}(k)\right| \exp\left\{i\hat{\theta}(k)\right\}, \tag{10.2.1}$$

where $\hat{f}(k)$ and $\hat{\theta}(k)$ are called the *amplitude spectrum* and the *phase spectrum*, respectively.

The *energy* (or *power*) spectrum of a signal is defined by

$$\hat{E}(k) = \left|\hat{f}(k)\right|^2, \tag{10.2.2}$$

so that the total energy of the signal $f(x)$ is given by

$$E = \int_{-\infty}^{\infty} \hat{E}(k)\, dk = \int_{-\infty}^{\infty} \left|\hat{f}(k)\right|^2 dk. \tag{10.2.3}$$

Clearly, it follows from (10.2.2) and (10.2.3) that the energy spectrum and the total energy depend only on the amplitude and are completely independent of the phase $\hat{\theta}(k)$. In other words, the Fourier transform does not provide any local or structural information on the signal. In spite of this major weakness, the Fourier transform has been useful to analyze stationary stochastic signals. In particular, the Fourier transform is fairly successful in the theory of a homogeneous turbulent velocity field confined within a box of volume a^3. In the case of three-dimensional turbulence, the Fourier transform of the velocity field $\mathbf{u}(\mathbf{x})$ has three components, each of the form $(j = 1, 2, 3)$,

$$\hat{u}_j(\mathbf{k}) = \frac{1}{(2\pi)^{3/2}} \int_{-\infty}^{\infty} \int_{-a/2}^{a/2} u_j(\mathbf{x}) \exp(i\mathbf{k} \cdot \mathbf{x}) d\mathbf{x}, \tag{10.2.4}$$

where $\hat{u}_j(\mathbf{k})$ can be expressed in terms of amplitude and phase by

$$\hat{u}_j(\mathbf{k}) = \left|\hat{u}_j(\mathbf{k})\right| \exp\left\{i\theta_j(\mathbf{k})\right\}. \tag{10.2.5}$$

Since $u_j(\mathbf{x})$ and $u_j(\mathbf{k})$ are random functions, it is necessary to define statistical quantities, of which the most important are the energy spectrum tensor $\Phi_{ij}(\mathbf{k})$ and cross correlation between components. Application of Fourier transforms shows that

$$\overline{\hat{u}_i^*(\mathbf{k})\, \hat{u}_j(\mathbf{k})} = \frac{1}{(2\pi)^{3/2}}\, a^3\, \Phi_{ij}(\mathbf{k}) \tag{10.2.6}$$

and

$$\overline{\hat{u}_i^*(\mathbf{k})\, \hat{u}_j(\mathbf{k}')} = \frac{1}{(2\pi)^{3/2}}\, \Phi_{ij}(\mathbf{k})\, \delta(\mathbf{k} - \mathbf{k}'), \tag{10.2.7}$$

where the bar represents an average over space and the asterisk denotes the complex conjugate. One of the most important properties of the turbulent flow is the correlation tensor of a homogeneous (stationary space $\mathbf{x}$) stochastic velocity field defined by

$$R_{ij}(\mathbf{r}, \mathbf{x}, t) = \overline{u_i(\mathbf{x})\, u_j(\mathbf{x} + \mathbf{r})}, \tag{10.2.8}$$

where $\mathbf{r}$ is the distance between simultaneous velocity fluctuations. Evidently

$$-\rho\, R_{ij}(0, \mathbf{x}, t) = -\rho\, \overline{u_i\, u_j} = \tau_{ij} \tag{10.2.9}$$

is called the *Reynolds stress tensor*.

The *energy spectrum tensor* in turbulence is defined as the Fourier transform of the covariance tensor $R_{ij}(\mathbf{r}, \mathbf{x}, t)$ by

$$\Phi_{ij}(\mathbf{k}\cdot\mathbf{x}, t) = \frac{1}{(2\pi)^{3/2}} \int_{-\infty}^{\infty} \exp(-i\mathbf{k}\cdot\mathbf{r})\, R_{ij}(\mathbf{r}, \mathbf{x}, t)\, d\mathbf{r}, \tag{10.2.10}$$

so that the inverse Fourier transform is given by

$$R_{ij}(\mathbf{r}, \mathbf{x}, t) = \frac{1}{(2\pi)^{3/2}} \int_{-\infty}^{\infty} \exp(i\mathbf{k}\cdot\mathbf{r})\Phi_{ij}(\mathbf{k}, \mathbf{x}, t)\, d\mathbf{k}, \tag{10.2.11}$$

where the integration is over all wavenumber $\mathbf{k}$-space. A spectrum tensor ψ_{ij} function of the single scale variable $k = |\mathbf{k}|$ can be obtained by averaging over all directions of the vector argument $\mathbf{k}$ so that

$$\psi_{ij}(k) = \int \Phi_{ij}(\mathbf{k})\, dS(k), \tag{10.2.12}$$

where this integration is taken in $\mathbf{k}$-space over a sphere of radius k of which $dS(k)$ is an element. The *energy* (*power*) *spectrum* is then defined by

$$E(k, t) = \frac{1}{(2\pi)^{3/2}} \Psi_{ii}(k) \tag{10.2.13}$$

so that the total energy $E = \frac{1}{2}\overline{u_i^2}$ is the integral of $E(k, t)$ over all k from 0 to ∞, that is,

$$\frac{1}{2}\overline{u_i^2} = \frac{1}{2}\int \Phi_{ii}(\mathbf{k})\, d(\mathbf{k}) = \int_0^{\infty} E(k, t)\, d(k). \tag{10.2.14}$$

Thus. it follows from (10.2.8) and (10.2.12) that

$$E(k, t) = \frac{1}{(2\pi)^{3/2}} \Psi_{ii}(k) = \frac{1}{(2\pi)^{3/2}} \int \Phi_{ii}(\mathbf{k})\, dS(k)$$

$$= \frac{1}{(2\pi)^{3/2}} \int \left|\hat{u}_i(\mathbf{k})\right|^2 dS(k). \tag{10.2.15}$$

The turbulent energy spectrum $E(k, t)$ represents the distribution of contributions to $\frac{1}{2}\overline{u_i^2}$ with respect to wavenumber (or scale) regardless of direction, and this is one of the most important characteristics of any turbulent (or three-dimensional wave) field. Thus. the study of the energy spectrum $E(k, t)$ is the central problem in the dynamics of turbulence. However, the information carried by the phase function $\theta_i(\mathbf{k})$ disappears completely in the definition of the energy spectrum.

One of the most common approaches to the study of turbulence is to use the Navier–Stokes equations together with the continuity equation in the Fourier transform space. In tensor notation, the Navier–Stokes equations for an unsteady motion of an incompressible viscous fluid of constant density ρ and kinematic viscosity ν and the continuity equation are

$$\frac{\partial u_i}{\partial t} + u_m \frac{\partial u_i}{\partial x_m} = -\frac{\partial p}{\partial x_i} + \nu \nabla^2 u_i + F_i, \tag{10.2.16}$$

$$\frac{\partial u_i}{\partial x_i} = 0, \tag{10.2.17}$$

where $u_i = u_i(\mathbf{x}, t)$ is the velocity field, p is the normal pressure divided by ρ, it is often called the *kinematic pressure*, and F_i are the external body forces. The continuity equation (10.2.17) is kinematic in nature and is unaffected by the energy dissipation process in the fluid due to viscosity.

It is important to point out that the use of the Navier–Stokes equations is perhaps justified for the study of turbulence because the Mach number of incompressible turbulent flows is relatively small.

Using the continuity equation (10.2.17), the Navier–Stokes equation (10.2.16) in the absence of the external field of forces ($F_i \equiv 0$) can be written as

$$\frac{\partial u_i}{\partial t} + \frac{\partial}{\partial x_m}(u_i\, u_m) = -\frac{\partial p}{\partial x_i} + \nu \nabla^2 u_i\,. \tag{10.2.18}$$

Taking the divergence of this equation and using (10.2.17) gives the Poisson equation

$$\nabla^2 p = -\frac{\partial^2 (u_i\, u_m)}{\partial x_i\, \partial x_m}. \tag{10.2.19}$$

Eliminating the pressure from the Navier–Stokes equations, we obtain

$$\frac{\partial u_i}{\partial t} - \nu \nabla^2 u_i = -\frac{1}{2} P_{ijm}(\nabla)(u_j\, u_m), \tag{10.2.20}$$

where

$$P_{ijm}(\nabla) = \frac{\partial}{\partial x_m} P_{ij}(\nabla) + \frac{\partial}{\partial x_j} P_{im}(\nabla), \tag{10.2.21}$$

$$\nabla = \left(\frac{\partial}{\partial x_1}, \frac{\partial}{\partial x_2}, \frac{\partial}{\partial x_3} \right), \tag{10.2.22}$$

and

$$P_{ij}(\nabla) = \delta_{ij} - \frac{1}{\nabla^2}\frac{\partial^2}{\partial x_i\,\partial x_j}. \tag{10.2.23}$$

The Fourier transform of the Navier–Stokes equations is

$$\left(\frac{\partial}{\partial t} + \nu k^2\right)\hat{u}_i(\mathbf{k},t) = -i\,k_m\,P_{ij}(\mathbf{k})\int u_j(\mathbf{q})\,u_m(\mathbf{k}-\mathbf{q})\,d^3\mathbf{q}, \tag{10.2.24}$$

where $\hat{u}_i(\mathbf{k},t)$ is the Fourier transform of $u_i(x_i,t)$, and

$$P_{ij}(\mathbf{k}) = \delta_{ij} - \frac{k_i\,k_j}{k^2}. \tag{10.2.25}$$

The velocity $u_i(\mathbf{x},t)$ is represented as a linear combination of plane waves, each corresponding to a characteristic size $O(k_i^{-1})$ in some direction i. However, the information related to position in physical space is completely hidden, which is a major drawback when dealing with the space of intermittency of turbulent flow. It has been recognized that turbulence has a set of localized structures, often called *coherent structures*, even at a very high Reynolds number $R = (U\ell/\nu)$ or at a very low viscosity. In many practical applications in aeronautics and meteorology, R varies in between 10^6 and 10^{12}. These coherent structures are organized spatial features, which repeatedly occur and undergo a characteristic temporal life cycle. There are many examples of such structures which play a central role in the time and space intermittency of turbulence. The classical model of turbulence is based on ensemble time or space average, but this idea is of no use for the description of coherent structure. On the other hand, the Navier–Stokes equations in physical space provide no explicit information about scales of motion. This information is often useful for modeling and physical insight into turbulent flows. This difficulty requires a representation that decomposes the flow field into contributions of different positions as well as different scales.

One of the most important features of a turbulent flow is the transfer of kinetic energy from large to small scales of motion due to the nonlinear (convective) term, which acts as the source of energy transfer. Denoting the nonlinear transfer of energy to wavenumbers of magnitude k by $T(k,t)$, the three-dimensional energy spectrum $E(k,t)$ for isotropic turbulence satisfies the evolution equation

$$\frac{\partial E}{\partial t} = T(k,t) - 2\nu k^2 E(k,t), \tag{10.2.26}$$

where $T(k,t)$ is formally defined in terms of triple products of fluctuating velocity and thus embodies the closure problem due to the nonlinear term in the Navier–Stokes equations. Equation (10.2.26) is made up of contributions of the inertial, nonlinear, and viscous terms of the Navier–Stokes equations. It follows from the

continuity equation (10.2.17) that the pressure term does not make any contribution to (10.2.26). This implies that the net effect of the pressure field is to conserve the total energy in the wavenumber space. Only the nonlinear term in the Navier–Stokes equations is responsible for the net energy transfer from large to smaller eddies or scales—a mechanism by which large eddies decay. The total spectral flux of energy through wavenumber k to all smaller scales is given by

$$\pi(k,t) = \int_k^\infty T(k',t)\,dk' = -\int_0^k T(k',t)\,dk', \tag{10.2.27}$$

so that

$$\int_0^\infty T(k',t)\,dk' = 0, \tag{10.2.28}$$

which also follows from the conservation of energy by the nonlinear term in (10.2.16). Consequently, the evolution equation (10.2.26) leads to

$$\frac{\partial}{\partial t}\left(\frac{1}{2}\overline{u_i\,u_i}\right) = \frac{\partial}{\partial t}\int_0^\infty E(k,t)\,dk = -\varepsilon(t), \tag{10.2.29}$$

and it follows from (10.2.26) that

$$\varepsilon(t) = 2\nu\int_0^\infty k^2 E(k,t)\,dk. \tag{10.2.30}$$

This clearly represents the overall rate of energy dissipation and exhibits that small-scale (or high wavenumbers) components are dissipated more rapidly by viscosity than large-scale (or low wavenumbers) components.

Based on the usual arguments of equilibrium and stationarity, it is easy to conclude that the ensemble average of the flux must equal to the overall rate of energy dissipation, so that $\langle\pi(k,t)\rangle_{ens} = \varepsilon(t)$ in the inertial range $\eta \ll k^{-1} \ll \ell$, where ℓ is the integral scale and η is the Kolmogorov microscale. Physically, the mechanism of energy transfer is described by simplified assumptions such as the successive breaking down of eddies or as the generation of small scales by the stretching and folding of vortices. Over the scales of motion of size k^{-1}, there is a net flux of kinetic energy to smaller scales that is equal to the time average of $\pi(k,t)$. However, $\pi(k,t)$ does not depend on *position* because the Fourier transform is used in the preceding analysis. This means that information related to position in physical space is completely absent in the theory of Kolmogorov (1941a,b), which neglects the phenomenon of intermittency.

It is also well known that the rate of dissipation $E(x,t)$ is distributed very intermittently—a feature which increases with the Reynolds number and its moments also increase with the Reynolds number according to power-laws in the inertial range (see Kolmogorov 1962). This allows a self-consistent statistical

and geometrical representation of ε in terms of multifractals (Benzi et al. 1984; Frisch and Parisi 1985). The power-law behavior of spatial moments of the energy dissipation can be modeled naturally within the framework of the breakdown of eddies with an additional assumption that the flux of energy to smaller scales shows spatial fluctuations. As the scales of motion become smaller, these spatial fluctuations accumulate and can then lead to very intermittent distributions of the energy dissipation. This clearly suggests that there is a need for defining a flux of kinetic energy instead of (10.2.27) which incorporates information on positions. In spite of these weaknesses of the Fourier analysis of turbulence, the upshot of the preceding description is that pressure and nonlinear inertial terms separately conserve the total energy of turbulence, whereas the linear viscous term dissipates the energy. Based on the assumption of self-similarity, Kolmogorov (1941a,b) and Oboukhov (1941) formulated a general statistical theory of turbulence, which is known as the *universal equilibrium theory*. This formulation represents a significant step in the development of the statistical theory of turbulence.

In order to study the energy spectrum function $E(k,t)$, Kolmogorov classified the spectrum into three major ranges, which are assumed to be independent. These ranges are called the large eddies ($kl \ll 1$), the energy containing eddies ($kl \sim 1$), and the small eddies ($kl \gg 1$), where l is the characteristic length scale of the energy-containing eddies or the differential length scale of the mean flow as a whole. For instance, the spectrum function $E(k,t)$ attains its maximum value at $k_l = l^{-1}$. The basic assumption of the Kolmogorov theory is that at a very high Reynolds number, the turbulent flow at the very small scales (large wavenumbers) is approximately similar to a state of statistical equilibrium and hence, this part of the spectrum is called the *equilibrium or quasi-equilibrium range*. Further, the motion of the small eddies is assumed to be statistically independent of that in the energy-containing range. The energy-containing scales of the motion may be inhomogeneous and anisotropic, but this feature is lost in the cascade so that at much smaller scales the motion is locally homogeneous and isotropic. Hence, the statistical properties of the turbulent motion in the equilibrium range must be completely determined by the physical parameters that are relevant to the dynamics of this part of the spectrum only. The motion associated with the equilibrium range ($kl \gg 1$) is uniquely determined only by two physical parameters, ε and ν. The consequence of this assumption is that the small-scale statistical characteristics of the velocity fluctuations in different turbulent flows with high Reynolds numbers can differ only by the length scales, which depend on ε and ν. According to the theory of Kolmogorov, the turbulent motion in the equilibrium range is dissipated by viscosity at the rate ε so that $E(k)$ is a function of ε, ν, and k. The net energy supply from the small wavenumbers is transferred by the nonlinear inertial interactions to larger and larger wavenumbers until the viscous dissipation becomes significant. Clearly, the Reynolds number must be very large for the existence of a statistical range of equilibrium. A necessary condition for this is $k_l \ll k_d$, where k_d is the location of the wavenumber at which the viscous dissipation first becomes dominant. In other words, the viscous dissipation takes place predominantly at the upper part of the equilibrium range, that is, at large wavenumbers $k \gg k_d \gg k_l$. Thus, for $R \gg 1$,

there exist two independent and widely separated regions $k \sim k_l$, (energy source) and near $k \sim k_d$ (energy sink), which are connected through a continuous set of wavenumbers k such that $k_l \ll k \ll k_d$. In other words, the Kolmogorov inertial range lies between the largest scale $l(l^{-1} = k_l)$, where the energy is supplied by external forces, and the smallest scales $d(d^{-1} = k_d)$, where the energy is dissipated by viscosity. This confirms the existence of an intermediate part of the energy spectrum, the so-called inertial range ($k_l \ll k \ll k_d$), where (a) the local energy transfer is significant, (b) the properties of the statistical ensemble are independent of all features of energy input except its rate, and (c) the viscous dissipation is insignificant. In this case, the nonlinear convection is quite significant, and the energy spectrum is therefore independent of viscosity v so that $E(k)$ depends only on ε and k. In a state of statistical equilibrium, the rate of energy input and the rate of energy dissipation. On a simple dimensional ground, the wavenumber spectrum of kinetic energy or the energy spectrum function in the inertial range takes the form

$$E(k) = C_k\, \varepsilon^{2/3} k^{-5/3} F\left(\frac{k}{k_d}\right), \tag{10.2.31}$$

provided $k \gg k_l$, and where C_k is a nondimensional universal parameter, called the *Kolmogorov constant*, $k_d = \left(\varepsilon/v^3\right)^{1/4}$ is the characteristic dissipation wavenumber and $F(x)$ is a universal dimensionless function. In homogeneous turbulence $\varepsilon \sim (u^3/l)$ (see Batchelor 1967), so that $k_d = \left(\frac{ul}{v}\right)^{3/4} k_l$. Clearly, $k_d \gg k_l$ is an essential requirement so that the Reynolds number $R = \left(\frac{ul}{v}\right)$ must be large. As R increases (or v decreases), the viscous dissipation would become predominant for larger and larger wavenumbers. According to Kolmogorov's hypothesis, for sufficiently large R there exists a significant range of wavenumbers with $k_l \ll k \ll k_d$, then, in this inertial range, both energy content and energy dissipation are negligible and the spectral energy flux $\varepsilon(k) = \varepsilon$ is independent of wavenumbers k. The molecular viscosity v then becomes insignificant, $F\left(\frac{k}{k_d}\right)$ in (10.2.31) becomes asymptotically constant for $k \ll k_d$, and then $F\left(\frac{k}{k_d}\right) \approx 1$. Consequently, the energy spectrum in the inertial range reduces to the form

$$E(k) = C_k\, \varepsilon^{2/3} k^{-5/3}. \tag{10.2.32}$$

This is called the *Kolmogorov–Oboukhov energy spectrum* in isotropic and homogeneous turbulence and received strong experimental support by Grant et al. (1962) in the early 1960s and later with a value of $C_k \approx 1.44 \pm 0.06$. Several experimental observations suggested that the spectrum power lies somewhere between $\frac{5}{3}$ and $\frac{7}{4}$. Even though the experimental accuracy is not very high, most experiments in

oceanic and atmospheric turbulence strongly support the $-\frac{5}{3}$ spectrum law. Very recently, Métais and Lesieur (1992) proposed the structure–function model of turbulence with the spectral eddy viscosity based upon a kinetic energy spectrum in space. Their analysis gives the best agreement with the Kolmogorov $k^{-5/3}$ spectrum law and the Kolmogorov constant $C_k \approx 1.40$.

Soon after Kolmogorov's pioneering work, considerable progress was made on a detailed study of different physical mechanisms of energy transfer of turbulence. Several authors including Heisenberg (1948a,b), Lin (1948), Chandrasekhar (1949, 1956), Batchelor (1967) , and Sen (1951, 1958), have investigated these problems. Of these physical energy transfer mechanisms, Heisenberg's eddy viscosity transfer was found to be more satisfactory at that time. Based on the assumption that the role of small eddies in the nonlinear transfer process is very much similar to that of molecules in viscous dissipation mechanisms, Heisenberg suggested that these small eddies act as an effective viscosity produced by the motions of the small eddies and the mean-square vorticity associated with the large eddies. He used this assumption to formulate the energy balance equation in the form

$$\frac{\partial}{\partial t}\int_0^k E(k,t)\,dt = -2\left(\nu + \frac{\eta_k}{\rho}\right)\int_0^k k^2 E(k,t)\,dk, \tag{10.2.33}$$

where η_k is the eddy viscosity defined by Heisenberg in the form

$$\eta_k = \rho\kappa \int_k^\infty \left\{\frac{E(k,t)}{k^3}\right\}^{1/2} dk, \tag{10.2.34}$$

where κ is a numerical constant.

Thus, the main problem of turbulence is to determine the spectrum function $E(k,t)$ satisfying the integro-differential equation (10.2.33) for all subsequent time when $E(k,t)$ is given at $t = 0$. For details of the problems, the reader is referred to Debnath (1978, 1998a,b).

10.3 Fractals, Multifractals, and Singularities in Turbulence

Mandelbrot (1982) first introduced the idea of a fractal as a self-similar geometric figure that consists of an identical motif repeating itself in an ever decreasing scale. This can be illustrated by the famous triadic Koch curve (see Fig. 10.1), which can be constructed geometrically by successive iterations. The construction begins with a line segment of unit length $\big(L(1) = 1\big)$, called the *initiator*. Divide it into three equal line segments. Then, replace the middle segment by an equilateral triangle without a base. This completes the first step $(n = 1)$ of the construction, giving a curve

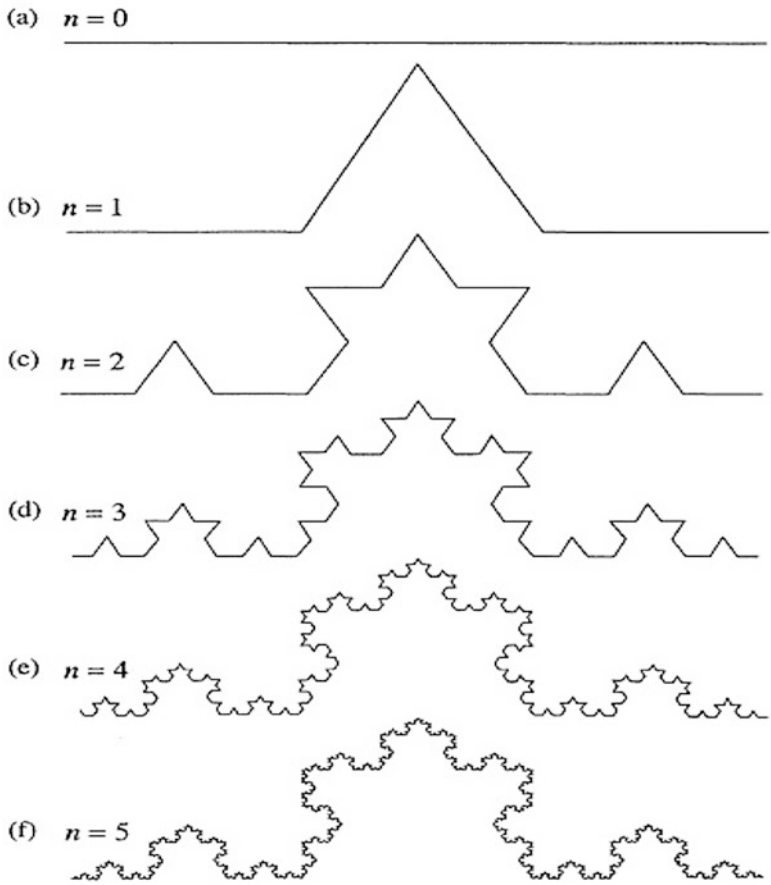

Fig. 10.1 The triadic Koch curve

of four line segments, each of length $\ell = \frac{1}{3}$, and the total length is $L\left(\frac{1}{3}\right) = \frac{4}{3}$. This new shape of the curve is called the *generator*. The second step ($n = 2$) is obtained by replacing each line segment by a scaled-down version of the generator. Thus, the second-generation curve consists of $N = 4^2$ line segments, each of length $\ell = \left(\frac{1}{3}\right)^2$, with the total length of the curve $L(\ell) = \left(\frac{4}{3}\right)^2$. Continuing this iteration process successfully leads to the triadic Koch curve of total length $L(\ell) = \left(\frac{4}{3}\right)^n$, where $\ell = 3^{-n}$, as shown in Fig. 10.1. The name *triadic* is justified because individual line segments at each step decrease in length by a factor of 3. Obviously, the Koch curve at the end of many iterations ($n \to \infty$) would have a wide range of scales. At any stage of the iteration process, the curve possesses several important

features. First, when a part of it is expanded by a factor of 3^n, it looks similar (except for reorientation) to that obtained in n previous steps. Second, self-similarity is built into the construction process. Third, there is no way to draw a tangent at each corner leading to a tangentless (or nondifferentiable) curve. Finally, this leads to the idea that self-similar fractals are invariant to dilation.

In terms of the box-counting algorithm in fractal geometry. the minimum $N(\ell) = 4$ boxes of size $\left(\frac{1}{3}\right)$ are needed to cover the line in the Koch curve in Fig. 10.1b. Similarly. at least $N(\ell) = 4^2$ boxes of size $\ell = \left(\frac{1}{3}\right)^2$ are required to cover the line in Fig. 10.1c. In general, a minimum of $N(\ell) = 4^n$ boxes of size $\ell = \left(\frac{1}{3}\right)^n$ are needed to cover the Koch curve obtained at the nth step. On the other hand, the total length $L(3^{-n}) = \left(\frac{4}{3}\right)^n$ at the nth iteration is obtained at a finer resolution of 3^{-n}. As the resolution increases microscopically ($n \to \infty$), the length of the Koch curve also increases without limit. This shows a striking contrast to an ordinary curve whose length remains the same for all resolutions. The intrinsic parameter that measures this property is called the *fractal Hausdorff dimension* D, which is defined by

$$D = \lim_{\ell \to 0} \frac{\log N(\ell)}{\log\left(\frac{1}{\ell}\right)} = \lim_{\ell \to 0} \frac{\log\left\{\frac{L(\ell)}{\ell}\right\}}{\log\left(\frac{1}{\ell}\right)}, \tag{10.3.1}$$

where $L(\ell) = \ell N(\ell) = \ell^{1-D}$ for small number ℓ.

For the triadic Koch curve, $N(\ell) = 4^n$ and $\ell = 3^{-n}$, so that its fractal dimension is given by

$$D = \frac{\log 4}{\log 3} \approx 1.2628 > 1 \tag{10.3.2}$$

and is noninteger and greater than one. The reason for this conclusion is due to the convolutedness of the Koch curve, which becomes more and more convoluted as the resolution becomes finer and finer. When the curve is highly convoluted, it effectively covers a two-dimensional area, that is, the one-dimensional curve fills up a space of dimension two. In general, a fractal surface has a dimension greater than two, and its dimension could become as large as three for a very highly convoluted surface, so that it can essentially cover a three-dimensional volume. This leads to a general result that the fractal Hausdorff dimension of a set is a measure of its space-filling ability.

Other famous examples include computer simulation of a diffusion-limited aggregation process, electrical discharges on insulators, which obey laws similar to diffusion-limited aggregation, and the resulting spark patterns. Computer simulations of such scale-invariant processes in three dimensions give a Hausdorff

dimension between two and three. One of the most remarkable three-dimensional highly branching lightnings has the Hausdorff dimension $D \approx 2.4$ or greater.

Mandelbrot (1982) also gave a more formal definition of a fractal as a set with Hausdorff dimension strictly greater than its topological dimension. This is similar to the Euclidean dimension of ordinary objects, but the fractal dimension D is noninteger and represents the basic measure of the space-filling ability of a fractal set. The topological dimension $E = 1$ for lines; for planes and surfaces, $E = 2$; and for spheres and other finite volumes, $E = 3$. In general, $D > E$, Mandelbrot also conjectured that fractals and the fractal Hausdorff dimension could be used effectively to model many phenomena in the real world.

While he was studying fractal geometry, Mandelbrot (1974) first recognized that the Kolmogorov statistical equilibrium theory of isotropic and homogeneous turbulence is essentially based on some basic assumptions, which include the hierarchy of self-similar eddies (or scales) of different orders and the energy cascade from larger and smaller eddies. This observation led him to believe that the structure of turbulence may be either locally or globally self-similar fractals. The problem of intermittency has also stimulated tremendous interest in the study of kinematics of turbulence using fractals and fractal dimensions (see Mandelbrot 1974, 1975). It is believed that the slow decay described by the Kolmogorov $k^{-5/3}$ law indicates a physical situation in which vortex sheets are infinitely convoluted. Mandelbrot recognized that these surfaces are so convoluted in the limit as $\nu \to 0$ as to occupy a space of fractal Hausdorff dimension between two and three. Then, he first proposed fractal analysis of turbulent flows and predicted that multiplicative cascade models, when continued indefinitely, lead to the dissipation of energy, which is confined to a set of non integer Hausdorff dimension. His fractal approach to turbulence received much attention after the introduction of a simple β-model by Frisch et al. (1978). They studied the β-model with special emphasis on its dynamical and fractal aspects. In addition, they explained both the geometrical and the physical significance of the fractal model of turbulent flows.

Experimental results of Anselmet et al. (1984) neither supported the β-model of Frisch nor the log-normal model of Kolmogorov. This meant that there was no uniform fractal model that could fully describe the complex structure of turbulent flows. Then, Frisch and Parisi (1985) have shown that intermittent distributions can be explained in terms of singularities of varying strength; all are located on interwoven sets of different fractal dimensions, and hence, Frisch and Parisi introduced the name *multifractals*. At the same time, Halsey et al. (1986) introduced $f(\alpha)$ for the fractal dimensions of sets of singularities characterizing multifractals. In their multifractal model of turbulence, they used the scale-invariance property, which is one of the remarkable symmetries of the Euler equations. In the meantime, the fractal facets of turbulence received considerable attention from Sreenivasan and Meneveau (1986) and Vassilicos (1992, 1993). Their analysis revealed some complicated geometric features of turbulent flows. They showed that several features of turbulence could be described approximately by fractals and that their fractal dimensions could be measured. Unfortunately, these studies can hardly prove that turbulence can be described fully by fractals. Indeed, these models now constitute a problem in

themselves in the sense that properties of turbulent flows can be used to find the value of fractal dimension D. Thus, fractal models of turbulence have not yet been fully successful.

Due to several difficulties with fractal models of turbulence, multifractal models with a continuous spectrum of fractal dimension $D(h)$ have been developed by several authors, including Meneveau and Sreenivasan (1987a,b) (p-model) and Benzi et al. (1984) (random β-model). These models produced scale exponents which are in agreement with experimental results with a single free parameter. However, it is important to point out that both the multifractal model and log-normal models lack true dynamical motivation. Recently, Frisch and Vergassola (1991) developed another multifractal model which enables them to predict a new form of universality for the energy spectrum $E(k)$ in the dissipation range. This model involves a universal function $D(h)$, called *fractal dimension*, which cannot be given by phenomenological theory. This new form of universal law has received good experimental support from Gagne and Castaing (1991), but it is not consistent with Kolmogorov's similarity hypothesis. They have analyzed a wide range of turbulence data with Reynolds numbers from 10^3 to 10^7.

Finally, we close this section by adding some comments on the possible development of singularities in turbulence. Mandelbrot (1975) has remarked that "the turbulent solutions of the basic equations involve singularities or 'near singularities' (approximate singularities valid down to local viscous length scales where the flow is regular) of an entirely new kind." He also stated that "the singularities of the solutions of the Navier-Stokes equations can only be fractals." In his authoritative review, Sreenivasan (1991) described the major influence of the fractal and multifractal formalisms in understanding certain aspects of turbulence, but he pointed out some inherent problems in these formalisms with the following comment, "However, the outlook for certain other aspects is not so optimistic, unless magical inspiration or breakthrough in analytical tools occur."

During the last decade, some progress has been made in the understanding of the implications of self-similar energy spectra of turbulence. It was shown by Thomson et al. (1879) in their study of oscillations that when the Fourier power spectrum of a function $f(x)$ has a self-similar form

$$E(k) \sim k^{-2p}, \tag{10.3.3}$$

where p is an integer, then there exists a discontinuity in the $(p-1)$ order derivative of $f(x)$. For example, the energy spectrum of a single shock $f(x) = \text{sgn}x$ is $E(k) \sim k^{-2}$ as $k \to \infty$. However, the energy spectrum such as $E(k) \sim k^{-2p}$, where p is not an integer, implies the existence of singularities that are more severe than mere discontinuities in the flow field. The singularity could be localized at one or a few points of the function such as $f(x) = \dfrac{\sin x}{x}$ (accumulating function) or could be global in the sense that $f(x)$ is singular at all or almost all x, as in the case of the Weierstrass function (see Falconer 1990). These two very different types of functions may have identical self-similar energy spectra of the form (10.2.3)

but always have *different phase spectra*. They also have a fractal (or K-fractal according to Vassilicos and Hunt's (1991) ideas) property in common; both are characterized by nontrivial Kolmogorov dimensions $D_K > 1, D'_K > 0$, where D_K is the Kolmogorov dimension of the entire function and D'_K is the Kolmogorov dimension of the intersection of a function with the x-axis, that is, the zero crossings. However, when the above two functions have the same energy spectrum similarity exponent p, they do not have the same values of D_K and D'_K. Moreover, their structure is also different in the Hausdorff sense, and the Hausdorff dimensions D_H and D'_H for the accumulating function are trivial in the sense that $D_H = 1$ and $D'_H = 0$, whereas those of the Weierstrass function are nontrivial, $D_H > 1$ and $D'_H > 0$. It has been conjectured by Mandelbrot (1982) that $D_H = D_K$ for H-fractals. Some of the major quantities involved in the statistical approach to turbulent flows are correlations and spectra. Self-similar cascades are usually associated with the power spectrum of the form

$$\Gamma(p) \sim k^{-p}. \tag{10.3.4}$$

For example, $p = 5/3$ corresponds to the Kolmogorov spectrum for small-scale turbulence, $p = 1$ characterizes the convective-inertial subrange, and $p = 5/3$ also corresponds to the Batchelor spectrum of a passive scalar in the inertial subrange. The question is whether the self-similarity leading to such spectra is *local* or *global*. Both local spectra are of the form (10.3.4) at large wavenumbers k, where p may not take integral values and p is related to the Kolmogorov dimension D_K of the interface, so that this relation can be used to derive the value of D_K in turbulence, which is in agreement with experimental findings. For a locally self-similar interface, the exponent $p = 2 - D'_K$, where D'_K is the Kolmogorov dimension of the interface with a linear cut, whereas for a globally self-similar interface, $p = 2 + E - D_H$, where E is the topological dimension and D_H is the Hausdorff dimension of the interface. Finally, it has been indicated by Vassilicos (1993) that the value of D_K may be a more accurate measure of spectra of locally self-similar interfaces than the direct measurement of the spectrum itself. Also, the value of D_K may be a more accurate criterion of high Reynolds number turbulence than the existence of self-similar spectra of the form (10.3.4). In the case of the Kolmogorov spectrum, $E(k) \sim k^{-5/3} (p = 5/6)$, which implies that the small-scale turbulence at a very high Reynolds number contains near-singularities that are either simple or nonisolated. Recent experimental findings and DNSs of turbulence have shown that the small scales of turbulent flows contain long and slender vortex tubes. Some of the vortex tubes may carry near-singularities, provided these vortex tubes are Lundgren vortices, which are asymptotic solutions of the Navier–Stokes equations in the limit as time $t \to \infty$. However, it has not yet been confirmed whether the picture of the small scales of turbulence where vortex tubes dominate the finest scales survives in the limit as $R \to \infty$.

Indeed, several theoretical works and experimental observations revealed that turbulence possesses some singularities in the velocity field or vorticity field. Sarker's (1985) analytical treatment confirmed that finite-time cusp singularities

always exist for essentially any arbitrary set of initial data and are shown to be generic. Newer experimental methods (Hunt and Vassilicos 1991) also provide evidence of spiraling streamlines and streaklines within eddies. and thin layers of large vorticity grouped together (Schwarz 1990); both of these features are associated with accumulation points in the velocity field. It also follows from solutions of the Navier–Stokes equations (Vincent and Meneguzzi 1991 and She et al. 1991) that very large deviations exist in isolated eddies with complicated internal structure. These studies identify regions of intense vorticity so that streamlines form spirals. The Kolmogorov inertial energy spectrum $k^{-5/3}$ also implies that there must be singularities in the derivatives of the velocity field on scales where the rate of energy dissipation is locally very large. It has been suggested by Moffatt (1984) that the accumulation points of discontinuities associated with spiral structures could give rise to fractional power laws k^{-2p} with $1 < 2p < 2$. The question also arises whether the self-similarity leading to the Kolmogorov spectrum is local or global. Moffatt's analysis (see Vassilicos 1992) revealed that spiral singularities are responsible for noninteger power of self-similar spectra k^{-2p}. It is also now known that locally self-similar structures have a self-similar high wavenumber spectrum with a noninteger power $2p$. Thus, the general conclusion is that functions with the Kolmogorov spectrum have some kinds of singularities and accumulation points, unless they are fractal functions with singularities everywhere, since they are everywhere continuous but nowhere differentiable. Thus, the upshot of this discussion is that the statistical structure of the small-scale turbulent flows is determined by local regions where the velocity and any other associated scalar functions have very large derivatives or have rapid variations in their magnitude or that of their derivatives. These are regions surrounding points that are singular. It remains an open question whether the nature of this singularity is due to random fluctuations of the turbulent motions resulting from their chaotic dynamics or to the presence of localized singular structures originating from an internal organization of the turbulent flows.

10.4 Farge's Wavelet Transform Analysis of Turbulence

It has already been indicated that the dynamics of turbulent flows depends not only on different length scales but on different positions and directions. Consequently, physical quantities such as energy, vorticity, enstrophy, and pressure become highly intermittent. The Fourier transform cannot give the local description of turbulent flows, but the wavelet transform analysis has the ability to provide a wide variety of local information of the physical quantities associated with turbulence. Therefore, the wavelet transform is adopted to define the space-scale energy density by

$$\tilde{E}(\ell, x) = \frac{1}{\ell} \left| \tilde{f}(\ell, x) \right|^2, \tag{10.4.1}$$

where $\tilde{f}(\ell, x)$ is the wavelet transform of a given function (or signal) $f(x)$.

It is helpful to introduce a *local energy spectrum* $\tilde{E}(\ell, x_0)$ in the neighborhood of x_0 (see Farge 1992) by

$$\tilde{E}_x(\ell, x_0) = \frac{1}{\ell} \int_{-\infty}^{\infty} \tilde{E}(\ell, x)\ \chi\left(\frac{x - x_0}{\ell}\right) dx, \tag{10.4.2}$$

where the function χ is considered as a filter around x_0. In particular, if χ is a Dirac delta function, then the local wavelet energy spectrum becomes

$$\tilde{E}(\ell, x_0) = \frac{1}{\ell} \left| \tilde{f}(\ell, x_0) \right|^2. \tag{10.4.3}$$

The local energy density can be defined by

$$\tilde{E}(x) = C_\psi^{-1} \int_0^{\infty} \tilde{E}(\ell, x)\, \frac{d\ell}{\ell}. \tag{10.4.4}$$

On the other hand, the *global wavelet spectrum* is given by

$$\tilde{E}(\ell) = \int_{-\infty}^{\infty} \tilde{E}(\ell, x)\, dx. \tag{10.4.5}$$

This can be expressed in terms of the Fourier energy spectrum $\hat{E}(k) = \left| \hat{f}(k) \right|^2$ so that

$$\tilde{E}(\ell) = \int_{-\infty}^{\infty} \tilde{E}(k) \left| \hat{\psi}(\ell k) \right|^2 dk, \tag{10.4.6}$$

where $\hat{\psi}(\ell k)$ is the Fourier transform of the analyzing wavelet ψ. Thus, the global wavelet energy spectrum corresponds to the Fourier energy spectrum smoothed by the wavelet spectrum at each scale.

Another significant feature of turbulence is the so-called intermittency phenomenon. Farge et al. (1992) used the wavelet transform to define the *local intermittency* as the ratio of the local energy density and the space averaged energy density in the form

$$I(\ell, x_0) = \frac{\left| \tilde{f}(\ell, x_0) \right|^2}{\left\langle \left\langle \left| \tilde{f}(\ell, x) \right|^2 \right\rangle \right\rangle}, \tag{10.4.7}$$

where

$$\left\langle \left\langle \left| \tilde{f}(\ell, x) \right|^2 \right\rangle \right\rangle = \int_{-\infty}^{\infty} \left| \tilde{f}(\ell, x) \right|^2 dx. \tag{10.4.8}$$

If $I(\ell, x_0) = 1$ for all ℓ and x_0, then there is no intermittency, that is, the flow has the same energy spectrum everywhere, which then corresponds to the Fourier energy spectrum. According to Farge et al. (1990a), if $I(\ell, x_0) = 10$, the point at x_0 contributes ten times more than average to the Fourier energy spectrum at scale ℓ. This shows a striking contrast with the Fourier transform analysis, which can describe a signal in terms of wavenumbers only but cannot give any local information. Several authors, including Farge and Rabreau (1988), Farge (1992), and Meneveau (1991) have employed wavelets to study homogeneous turbulent flows in different configurations. They showed that during the flow evolution, beginning from a random vorticity distribution with a k^{-3} energy spectrum, the small scales of the vorticity become increasingly localized in physical space. Their analysis also revealed that the energy in the two-dimensional turbulence is highly intermittent which may be due to a condensation of the vorticity field into vortex like coherent structures. They have also found that the smallest scales of the vorticity are confined within vortex cores. According to Farge and Holschneider (1989, 1990), there exist quasisingular coherent structures in two-dimensional turbulent flows. These kinds of structures are produced by the condensation of vorticity around the quasisingularities already present in the initial data. Using the wavelet transform analysis, Meneveau (1991) first measured the local energy spectra and then carried out DNSs of turbulent shear flows. His study reveals that the mean spatial values of the turbulent shear flow agree with their corresponding results in Fourier space, but their spatial variations at each scale are found to be very large, showing non-Gaussian statistics. Moreover, the local energy flux associated with very small scales exhibits large spatial intermittency. Meneveau's computational analysis of the spatial fluctuations of $T(k, t)$ shows that the average value of $T(k, t)$ is positive for all small scales and negative for large scales, indicating the transfer of energy from large scales to small scales so that energy is eventually dissipated by viscosity. This finding agrees with the classical cascade model of three-dimensional turbulence. However, there is a striking new phenomenon that the energy cascade is reversed in the sense that energy transfer takes place from small to large scales in many places in the flow field. Perrier et al. (1995) confirmed that the mean wavelet spectrum $\tilde{E}(k)$ is given by

$$\tilde{E}(k) = \int_0^\infty \tilde{E}(x, k)\, dx. \tag{10.4.9}$$

This result gives the correct Fourier exponent for a power-law of the Fourier energy spectrum $E(k) = Ck^{-p}$, provided the associated wavelet has at least $n > 2^{-1}(p-1)$ vanishing moments. This condition is in agreement with that for determining cusp singularities. Based on a recent wavelet analysis of a numerically calculated two-dimensional homogeneous turbulent flow, Benzi and Vergassola (1991) confirmed the existence of coherent structures with negative exponents. Thus, their study reveals that the wavelet transform analysis has the ability not only to give a more precise local description but also detect and characterize singularities of turbulent flows. On the other hand, Argoul et al. (1988, 1990) and Everson et al.

(1990) have done considerable research on turbulent flows using wavelet analysis. They showed that the wavelet analysis has the ability to reveal Cantor-like fractal structure of the Richardson cascade of turbulent eddies.

10.5 Adaptive Wavelet Method for Analysis of Turbulent Flows

Several authors, including Farge (1992) and Schneider and Farge (1997), first introduced the adaptive wavelet method for the study of fully developed turbulence in an incompressible viscous flow at a very high Reynolds number. In a fully developed turbulence, the nonlinear convective term in the Navier–Stokes equations becomes very large by several orders of magnitude than the linear viscous term. The Reynolds number $R = \left(U\ell/v\right)$ represents the ratio of the nonlinear convective term and the viscous term. In other words, R is proportional to the ratio of the large excited scales and the small scales where the linear viscous term is responsible for dissipating any instabilities.

Unpredictability is a key feature of turbulent flows, that is, each flow realization is different even though statistics are reproducible as long as the flow configuration and the associated parameters remain the same. Many observations show that in each flow realization localized coherent vortices whose motions are chaotic are generated by their mutual interactions. The statistical analysis of isotropic and homogeneous turbulence is based on L^2-norm ensemble averages and hence is hardly sensitive to the presence of coherent vortices which have a very weak contribution to the L^2-norm. However, coherent vortices, are fundamental components of turbulent flows and therefore, must be taken into account in both statistical and numerical models.

Leonard (1974) developed a classical model, called the *Large Eddy Simulation* (LES), to compute fully developed turbulent flows. In this model, separation is introduced by means of linear filtering between large-scale active modes and small-scale passive modes. This means that the flow evolution is calculated deterministically up to cutoff scale while the influence of the subgrid scales onto the resolved scales is statistically modeled. Consequently, vortices in strong nonlinear interaction tend to smooth out, and any instabilities at subgrid scales are neglected. Thus, LES models have problems of backscatter, that is, transfer of energy from subgrid scales to resolved scales due to nonlinear instability. The LES model takes into account backscatter, but only in a locally averaged manner. Further progress in the hierarchy of turbulent models is made by using Reynolds Averaged Navier–Stokes (RANS) equations, where the time averaged mean flow is calculated and fluctuations are modeled, in this case, only steady state solutions are predicted.

During the last decade, wavelet analysis has been introduced to model, analyze, and compute fully developed turbulent flows. According to Schneider and Farge (2000), wavelet analysis has the ability to disentangle coherent vortices from incoherent background flow in turbulent flows. These components are inherently

multiscale in nature and have different statistics with different correlations. Indeed, the coherent vortices lead to the non-Gaussian distribution and long-range correlations, whereas the incoherent background flow is inherently characterized by the Gaussian statistics and short-range correlations. This information suggests a new way of splitting the turbulent flow into active coherent vortex modes and passive incoherent modes. The former modes are computed by using wavelet analysis, whereas the latter modes are statistically modeled as a Gaussian random process. This new and modem approach is called the *Coherent Vortex Simulation* (CVS) and was developed by Farge et al. (1999a,b). This approach is significantly different from the classical LES which is essentially based on a linear filtering process between large and small scales without any distinction between Gaussian and non-Gaussian processes. The CVS takes advantage of a nonlinear filtering process defined in a wavelet space between Gaussian and non-Gaussian modes with different scaling laws but without any scale separation. The major advantage of the CVS treatment compared to the LES is to reduce the number of computed active modes for a given Reynolds number and control the Gaussian distribution of the passive degrees of freedom to be statistically modeled.

Turbulent flows are characterized by a fundamental quantity, called the *vorticity vector*, $\boldsymbol{\omega} = \nabla \times \mathbf{u}$. Physically, the vorticity field is a measure of the local rotation rate of the flow, its angular velocity.

Eliminating the pressure term from (10.2.16) by taking the curl of (10.2.16) leads to the equation for the vorticity field in the form

$$\frac{\partial \boldsymbol{\omega}}{\partial t} = (\boldsymbol{\omega} \cdot \nabla)\mathbf{u} - (\mathbf{u} \cdot \nabla)\boldsymbol{\omega} + \nu \nabla^2 \boldsymbol{\omega} + \nabla \times \mathbf{F}. \tag{10.5.1}$$

This is well known as the *convection–diffusion equation* of the vorticity. The left-hand side of this equation represents the rate of change of vorticity, whereas the first two terms on the right-hand side describe the rate of change of vorticity due to stretching and twisting of vortex lines. In fact, the term $(\boldsymbol{\omega} \cdot \nabla)\mathbf{u}$ is responsible for the vortex-stretching mechanism (vortex tubes are stretched by velocity gradients) which leads to the production of vorticity. The third term on the right-hand side of (10.5.1) represents the diffusion of vorticity by molecular viscosity. In the case of two-dimensional flow, $(\boldsymbol{\omega} \cdot \nabla)\mathbf{u} = 0$, so the vorticity equation (10.5.1) without any external force can be given by

$$\frac{\partial \boldsymbol{\omega}}{\partial t} + (\mathbf{u} \cdot \nabla)\boldsymbol{\omega} = \nu \nabla^2 \boldsymbol{\omega} \tag{10.5.2}$$

so that only convection and conduction occur. This equation combined with the equation of continuity,

$$\nabla \cdot \mathbf{u} = 0, \tag{10.5.3}$$

constitutes a closed system which is studied by periodic boundary conditions.

In terms of a stream function ψ, the continuity equation (10.5.3) gives

$$u = \frac{\partial \psi}{\partial y} \quad \text{and} \quad v = -\frac{\partial \psi}{\partial x}, \tag{10.5.4a,b}$$

so that the vorticity $\omega = (v_x - u_y)$ satisfies the Poisson equation for the stream function ψ as

$$\nabla^2 \psi = \omega. \tag{10.5.5}$$

The total kinetic energy is defined by

$$E(t) = \frac{1}{2} \iint_D \mathbf{u}^2(x,t)\, dx, \tag{10.5.6}$$

and the total enstrophy is defined by

$$Z(t) = \frac{1}{2} \iint_D \boldsymbol{\omega}^2(x,t)\, dx. \tag{10.5.7}$$

We make reference to Frisch (1995) to express the enstrophy and the dissipation of energy as

$$\frac{dZ}{dt} = -2vP, \quad \frac{dE}{dt} = -2vZ, \tag{10.5.8a,b}$$

where the *palinstrophy* P is given by

$$P(t) = \frac{1}{2} \iint_D \left|\nabla \boldsymbol{\omega}\right|^2 dx. \tag{10.5.9}$$

The energy and enstrophy spectra are written in terms of the Fourier transform

$$E(\kappa) = \frac{1}{2} \sum_{\kappa - \frac{1}{2} \le |\mathbf{k}| \le \kappa + \frac{1}{2}} \left|\hat{u}(\mathbf{k})\right|^2, \tag{10.5.10}$$

$$Z(\kappa) = \frac{1}{2} \sum_{\kappa - \frac{1}{2} \le |\mathbf{k}| \le \kappa} \left|\hat{\omega}(\mathbf{k})\right|^2, \tag{10.5.11}$$

where $\mathbf{k} = (k, \ell)$. The quantities $E(\kappa)$ and $Z(\kappa)$ measure the amount of energy or enstrophy in the band of wavenumbers between κ and $\kappa + d\kappa$. The spectral distribution of energy and enstrophy are related to the expression $\kappa^2 E(\kappa) = Z(\kappa)$.

During the last two decades, several versions of the DNS have been suggested to describe the dynamics of turbulent flows. Using DNS, the evolution of all scales of

turbulence can only be computed for moderate Reynolds numbers with the help of supercomputers. Due to severe limitations of DNS, Fröhlich and Schneider (1997) have recently developed a new method, called the *adaptive wavelet method*, for simulation of two- and three-dimensional turbulent flows at a very high Reynolds number. This new approach seems to be useful for simulating turbulence because the inherent structures involved in turbulence are localized coherent vortices evolving in multiscale nonlinear dynamics. Fröhlich and Schneider used wavelet basis functions that are localized in both physical and spectral spaces, and hence the approach is a reasonable compromise between grid-point methods and spectral methods. Thus, the space and space-adaptivity of the wavelet basis seem to be effective. The fact that the basis is adapted to the solution and follows the time evolution of coherent vortices corresponds to a combination of both Eulerian and Lagrangian methods. Subsequently, Schneider and Farge (2000) discussed several applications of the adaptive wavelet method to typical turbulent flows with computational results for temporally growing mixing layers, homogeneous turbulent flows, and for decaying and wavelet forced turbulence. They used the adaptive wavelet method for computing and analyzing two-dimensional turbulent flows. At the same time, they discussed some perspectives for computing and analyzing three-dimensional turbulent flows with new results. They also have shown that the adaptive wavelet approach provides highly accurate results at high Reynolds numbers with many fewer active modes than the classical pseudospectral method, which puts a limit on the Reynolds numbers because it does not utilize the vortical structure of high Reynolds number flows. The reader is referred to all papers cited above for more detailed information on the adaptive wavelet method for computing and analyzing turbulent flows.

10.6 Meneveau's Wavelet Analysis of Turbulence

In this section, we closely follow Meneveau's (1991) analysis of turbulence in the orthonormal wavelet representation based on the wavelet transformed Navier–Stokes equations. We first introduce the three-dimensional wavelet transform of a function $f(\mathbf{x})$ defined by

$$w(r,\mathbf{x}) = W^{[f]}_{(r,\mathbf{x})} = \frac{r^{-3/2}}{\sqrt{C_\psi}} \int_{-\infty}^{\infty} \psi\left(\frac{\boldsymbol{\xi}-\mathbf{x}}{r}\right) f(\boldsymbol{\xi})\, d^3\boldsymbol{\xi}, \tag{10.6.1}$$

where $\psi(\mathbf{x}) = \psi\big(|\mathbf{x}|\big)$ is the isotropic wavelet satisfying the admissibility condition

$$C_\psi = \int_{-\infty}^{\infty} |\mathbf{k}|^{-1} \left|\hat{\psi}(\mathbf{k})\right|^2 d^3\mathbf{k}. \tag{10.6.2}$$

The inversion formula is given by

$$f(\mathbf{x}) = \frac{1}{\sqrt{C_\psi}} \int_{-\infty}^{\infty} dr \int_{-\infty}^{\infty} r^{-3/2}\, \psi\left(\frac{\mathbf{x}-\boldsymbol{\xi}}{r}\right) w(r,\boldsymbol{\xi})\, \frac{d^3\boldsymbol{\xi}}{r^4}. \tag{10.6.3}$$

The invariance of energy of the system can be stated as

$$\int_{-\infty}^{\infty} \{f(\mathbf{x})\}^2 d^3\mathbf{x} = C_\psi^{-1} \int_0^{\infty} dr \int_{-\infty}^{\infty} \{w(r,\mathbf{x})\}^2\, \frac{d^3\mathbf{x}}{r^4}. \tag{10.6.4}$$

As in the one-dimensional case, the wavelet transform $w(r,x)$ can also be obtained from the Fourier transform $\hat{f}(\mathbf{k})$ of $f(\mathbf{x})$ so that

$$w(r,\mathbf{x}) = \frac{1}{(2\pi)^3} \frac{1}{\sqrt{C_\psi}}\, r^{3/2} \int_{-\infty}^{\infty} \hat{\psi}^*(r\mathbf{k})\, \hat{f}(\mathbf{k})\, e^{i(\mathbf{k}\cdot\mathbf{x})}\, d^3\mathbf{k}. \tag{10.6.5}$$

This can also be inverted to obtain the inversion formula

$$\hat{f}(\mathbf{k}) = \frac{1}{\sqrt{C_\psi}} \int_0^{\infty} dr \int_{-\infty}^{\infty} r^{3/2}\, \hat{\xi}(r\mathbf{k})\, \exp(-i\mathbf{k}\cdot\mathbf{x}) w(r,\mathbf{x})\, \frac{d^3\mathbf{x}}{r^4}. \tag{10.6.6}$$

In view of the translational property, the wavelet transform commutes with differentiation in the space variables so that

$$\nabla \cdot \mathbf{W}_{(r,\mathbf{x})}[\mathbf{f}] = W_{(r,\mathbf{x})}[\nabla \cdot \mathbf{f}] \tag{10.6.7}$$

and

$$\nabla\, \mathbf{W}_{(r,\mathbf{x})}[\mathbf{f}] = W_{(r,\mathbf{x})}[\nabla\, \mathbf{f}]. \tag{10.6.8}$$

We now define $w_i(r,\mathbf{x})$ as the wavelet transform of the fluctuating part of the divergence-free velocity field $u_i(\mathbf{x})$. In vector notation, these quantities are denoted by $\mathbf{w}(r,\mathbf{x})$ and $\mathbf{u}(\mathbf{x})$, which depend on time t, but for notational clarity, we simply omit the time dependence. It follows from (10.6.7) that $\mathbf{w}(r,\mathbf{x})$ is divergence-free.

We apply (10.6.5) to the Fourier-transformed Navier–Stokes equations (10.2.24), where the velocities on the right-hand side have been replaced by the inverse transform of $w_i(r,\mathbf{x})$, so that the evolution equation for $w_i(r,\mathbf{x})$ is

$$\left(\frac{\partial}{\partial t} - \nu\nabla^2\right) w_i(r,x) = \frac{1}{\left(2\pi C_\psi\right)^{3/2}} \int_{r'} dr' \int_{r''} dr'' \int_{\mathbf{x}'} \int_{\mathbf{x}''} w_j(r',\mathbf{x}')\, w_k(r'',\mathbf{x}'') I_{ijk}(r,\mathbf{x};r',r'',\mathbf{x}',\mathbf{x}'')\, \frac{d^3\mathbf{x}' d^3\mathbf{x}''}{r'^4\, r''^4}, \tag{10.6.9}$$

where

$$I_{ijk}(r,\mathbf{x};r',r'',\mathbf{x}',\mathbf{x}'') = (-i)\left(rr'r''\right)^{3/2}\int_k\int_q k_k P_{ij}(\mathbf{k})\,\hat{\psi}^*(r\mathbf{k})\,\hat{\psi}(r'\mathbf{q}) \times \hat{\psi}\left\{r''(\mathbf{k}-\mathbf{q})\right\}\exp\left[i\left\{\mathbf{k}\cdot(\mathbf{x}-\mathbf{x}'')+q\cdot(\mathbf{x}''-\mathbf{x}')\right\}\right]d^3\mathbf{k}\,d^3\mathbf{q}. \tag{10.6.10}$$

We multiply (10.6.9) by $w_i(r,\mathbf{x})$ and then add over the components I to obtain the local energy equation

$$\frac{\partial}{\partial t}e(r,\mathbf{x}) = t(r,\mathbf{x}) - \varepsilon(r,\mathbf{x}) + \nu\frac{\partial}{\partial x_j}\left[w_i\left(\frac{\partial w_i}{\partial x_j}+\frac{\partial w_j}{\partial x_i}\right)\right], \tag{10.6.11}$$

where

$$e(r,\mathbf{x}) = \frac{1}{2}\sum_{i=1}^{3}\left[w_i(r,\mathbf{x})\right]^2 \tag{10.6.12}$$

represents the local density of kinetic energy at scale r and

$$t(r,\mathbf{x}) = \int dr'\int dr''\iint w_i(r,\mathbf{x})\,w_j(r',\mathbf{x}')\,w_k(r,\mathbf{x}'') \times I_{ijk}(r,\mathbf{x};r',r'',\mathbf{x}',\mathbf{x}'')\,\frac{d^3\mathbf{x}'d^3\mathbf{x}''}{r'^4\,r''^4}, \tag{10.6.13}$$

is the local transfer of kinetic energy at scale r at position $\mathbf{x}$. This term shows interactions among triads of scales (r,r',r'') as well as interactions among triads of positions $(\mathbf{x},\mathbf{x}',\mathbf{x}'')$. The term $\varepsilon(r,\mathbf{x})$ describes the dissipation of energy at scale size r and is given by

$$\varepsilon(r,\mathbf{x}) = \nu\frac{\partial w_i}{\partial x_j}\left[\frac{\partial w_i}{\partial x_j}+\frac{\partial w_j}{\partial x_i}\right]. \tag{10.6.14}$$

In view of the Parseval formula (6.3.9), the local transfer conserves energy so that

$$\int_r dr\int_{\mathbf{x}} t(r,\mathbf{x})\,\frac{d^3\mathbf{x}}{r^4} = 0. \tag{10.6.15}$$

The total flux of kinetic energy through scale r at position $\mathbf{x}$ is defined by integrating the rate of change in the local energy due to nonlinear interactions over all scales larger than r so that

$$\pi(r,\mathbf{x}) = -\int_r^\infty t(r',\mathbf{x})\,\frac{dr'}{r'^4}, \tag{10.6.16}$$

where the negative sign shows a decrease in energy of the large scales associated with a positive flux. This total flux term is somewhat similar to (10.2.27) in the wavelet representation.

All the preceding results are not very useful in turbulence theory, but they illustrate the fact that there are complicated interactions of the wavelet transform $w_i(r, \mathbf{x})$ involved at different scales and different positions. These nonlocal and interscale interactions are essentially described by the complicated quantity $I_{ijk}(r, \mathbf{x}; r', r'', \mathbf{x}', \mathbf{x}'')$. This quantity arises from the fact that, in general, the triads are not closed as they are in the Fourier representation, that is, there is no detailed energy conservation in the wavelet representation. However, it is almost impossible to make further progress on this wavelet formulation without making appropriate assumptions and approximations of I_{ijk}.

On the other hand, if the velocity field is known, quantities including $e(r, \mathbf{x}), t(r, \mathbf{x})$, and $\pi(r, \mathbf{x})$ can be computed by taking the wavelet transform of the Navier–Stokes equation combined with expressing the nonlinear terms in terms of the original velocity field. Meneveau (1991) described the discrete formulation of the evolution equation for the local kinetic energy density $e^{(m)}[\mathbf{i}]$ at scale r_m and position $y = 2^m(h_1 i_1, h_2 i_2, h_3 i_3)$ where $\mathbf{i} = (i_1, i_2, i_3)$ denotes the position of a rectangular grid with uniform mesh sizes h_1, h_2, h_3. He obtained the evolution equation for the local kinetic energy density $e^{(m)}[\mathbf{i}]$ given by

$$\frac{\partial}{\partial t} e^{(m)}[\mathbf{i}] = t^{(m)}[\mathbf{i}] - \nu^{(m)}[\mathbf{i}], \tag{10.6.17}$$

where $t^{(m)}[\mathbf{i}]$ is the nonlinear term representing the local transfer of kinetic energy at scales r_m at position $\mathbf{i}$, and $\nu^{(m)}[\mathbf{i}]$ is the viscous term representing dissipation and viscous transport of kinetic energy. Equation (10.6.17) is somewhat similar to (10.2.27), but it depends on the position as well.

We write the expressions for $t^{(m)}[\mathbf{i}]$ as

$$t^{(m)}[\mathbf{i}] = -\sum_{i=1}^{3} \sum_{q=1}^{7} w_i^{(m,q)}[\mathbf{i}] \left\{ u_j \frac{\partial u_i}{\partial x_j} + \frac{1}{\rho} \frac{\partial p}{\partial x_i} \right\}^{(m,q)} [\mathbf{i}], \tag{10.6.18}$$

where the pressure involved in this equation is obtained by solving the Poisson equation, and $w_i^{(m,q)}[\mathbf{i}]$ is the wavelet coefficient of the ith component of the velocity field.

The term $t^{(m)}[\mathbf{i}]$ does conserve energy on the whole so that

$$\sum_{m=1}^{M} \sum_{i_1, i_2, i_3} t^{(m)}[\mathbf{i}] = 0, \tag{10.6.19}$$

which follows from the zero value of the volume integral of $(\mathbf{u} \cdot \nabla \mathbf{u} + \nabla p)$ for homogeneous turbulence, and from the condition of orthonormality of the wavelets.

The viscous term is given by

$$v^{(m)}[\mathbf{i}] = v \sum_{i=1}^{3} \sum_{q=1}^{7} w_i^{(m,q)}[\mathbf{i}] \left\{-\nabla^2 u_i\right\}^{(m,q)}[\mathbf{i}]. \tag{10.6.20}$$

Finally, the flux of the kinetic energy term $\pi^{(m)}[\mathbf{i}]$ in a spatial region of size r_m and position $[\mathbf{i}]$ can be calculated by summing the density transfer of all larger scales at that position so that

$$\pi^{(m)}[\mathbf{i}] = -\sum_{n=m}^{M} 2^{3(M-n)}\, t^{(n)}\left[2^{m-n}\mathbf{i}\right]. \tag{10.6.21}$$

We next characterize the local kinetic energy at every scale in turbulence. In Fourier transform analysis, the quantity $\hat{E}(k)$ represents the power-spectral density in a band dk of wavenumbers. However, the spatial information is completely lost due to the nonlocal nature of the Fourier modes. If $u(x)$ is a one-dimensional finite energy function with mean zero and $\hat{u}(k)$ is its Fourier transform, the total energy is given by

$$\int_{-\infty}^{\infty} u^2(x)\, dx = \frac{1}{2\pi} \int_{-\infty}^{\infty} \hat{u}(k)\, \hat{u}^*(k)\, dk = \int_0^{\infty} E(k)\, dk, \tag{10.6.22}$$

where $E(k)$ represents the energy spectrum, and the wavenumber k is related to the distance r so that $r = 2\pi k$.

In wavelet analysis, the total energy can be written in terms of the wavelet energies in the form

$$\int_{-\infty}^{\infty} u^2(x)\, dx = \int_0^{\infty} E_w(k)\, dk, \tag{10.6.23}$$

where $E_w(r, x)$ is the continuous wavelet transform of $u(x)$ and

$$E_w(k) = \frac{1}{2\pi} \frac{1}{C_\psi} \int_{-\infty}^{\infty} w^2\big(r(k), x\big)\, dx. \tag{10.6.24}$$

This represents the energy density at wavenumbers k. This spectrum function is similar to the Fourier spectrum $E(k)$ but is not the same at each k because of the finite bandwidth involved in the wavelet transform.

For more detailed information on energy transfer and flux in the wavelet representation and the intermittent nature of the energy, the reader is referred to Meneveau (1991).